

TRAJECTORY UNCERTAINTY IN REPEAT-PASS SAR INTERFEROMETRY: A CASE STUDY

Roberto Coscione¹, Irena Hajnsek^{1,2}, Othmar Frey^{1,3}

¹Earth Observation and Remote Sensing, ETH Zurich, Switzerland

²Microwaves and Radar Institute, German Aerospace Center - DLR, Oberpfaffenhofen, Germany

³Gamma Remote Sensing AG, Gümüli, Switzerland

ABSTRACT

In the context of differential synthetic aperture radar interferometry (DInSAR), precise trajectory estimation of the SAR platform is necessary to minimize residual phase errors induced by inaccurate knowledge of the 3D acquisition geometry.

Inertial navigation systems (INS) and global navigation satellite system (GNSS) are usually employed to track the position of the platform. However, their unavoidable inaccuracies lead to motion estimation errors that negatively affect the quality of the processed radar data.

To assess the positioning performance in a repeat-pass scenario, we used a navigation-grade INS/GNSS system to precisely track the position and the attitude of a platform moving along a rail and carrying a SAR sensor. We analyse the performance of the positioning solution for different scenarios relevant to repeat-pass DInSAR. Since the position of the platform is nearly perfectly repeated at every pass (zero interferometric baseline), the precision of the estimated position can be assessed and the interferometric performance evaluated.

Index Terms— Radar, interferometry, DInSAR, terrestrial SAR, inertial navigation system (INS), global navigation satellite system (GNSS), real time kinematic (RTK), post-processed kinematic (PPK)

1. INTRODUCTION

Terrestrial radar systems are often employed to monitor surfaces and structures subject to surface displacement over time, such as landslides, glaciers, mines, etc. [1], usually by means of differential synthetic aperture radar interferometry (DInSAR) [2]. Their value comes especially from the geometry of acquisition suitable for steep slopes and the flexible temporal baselines, two areas in which spaceborne systems have inherent limitations.

A limitation of the terrestrial systems is the range-dependent azimuth resolution, specifically at low frequency, due to the limited dimension of the synthetic antenna. Airborne systems, which are not affected by this problem, are

mainly limited by the high operational cost. A possible solution is offered by a car-borne SAR system [3, 4, 5] with which is possible to achieve synthetic apertures of hundreds of meters, high azimuth resolution independent from the range, and flexible temporal baselines at relatively low operational cost.

However, similarly to the airborne case, the usability of the car-borne system for deformation monitoring is challenged by the presence of errors in the estimated trajectory, which cause image degradation and spectral distortions [6, 7].

Trajectories are usually measured by means of inertial navigation systems (INS) and global navigation satellite systems (GNSS). However, INS/GNSS systems present unavoidable inaccuracies whose magnitude is linked to the performance of the equipment, to the satellite coverage, and to the processing configuration adopted. This is particularly relevant when the integration time of the SAR system is on the order of minutes, such as in the car-borne scenario, and hence time-dependent non-linear deviations from the real trajectory can be experienced.

Precise trajectory estimation of the SAR platform is necessary not only to correctly focus the radar images but especially to minimize the phase errors induced by inaccurate knowledge of the 3D acquisition geometry. This is particularly relevant in a car-borne or UAV-borne measurement setup where the radar may be moving in relatively close range distances from the area of interest.

Although auto-focusing and motion compensation techniques can be employed [8, 9, 10], availability of high-quality positioning data is crucial to minimize the phase errors. Through accurate knowledge of the repeat-pass trajectories, which translates into accurate knowledge of the azimuth-varying interferometric baseline, the residual phase variations are reduced to smoothly varying linear function or low-order polynomial functions.

To assess the positioning performance in a repeat-pass scenario, we performed positioning measurements with a navigation-grade INS/GNSS system of a SAR sensor moving along a rail. We analyse the performance of the positioning solution for different scenarios relevant to DInSAR applications. Since the position of the platform is nearly perfectly

repeated at every pass (zero interferometric baseline), the precision of the estimated position can be precisely assessed and the interferometric performance evaluated.

The measurement campaign took place in July 2018 in the Bernese Alps where radar acquisitions of the Steingletscher (Stein glacier) have been performed.

2. MEASUREMENT SETUP

The radar and the INS/GNSS system are mounted on a platform moving along a rail at slow speed (40 cm/s on a quasi-linear trajectory). L-band radar acquisitions are performed at every pass during the forward movement of the platform.

The INS is a navigation-grade system (iMAR iNAV-RQH-10018) with free inertial position accuracy below 0.6 nm/h (nautical miles per hour).

A portable GNSS receiver (indicated as local station in the following) is steadily positioned few meters away from the rail. Such receiver is equipped with a geodetic antenna with bottom shielding to reduce multipath, is dual-frequency, and operates in static mode.

The local reference station is used to provide an approximately atmosphere-free post-processed kinematic GNSS solution which is then compared to the solutions obtained with permanent GNSS stations positioned tens of kilometers away from the test site and at different altitudes.

3. RTK/PPK PROCESSING AND INS/GNSS INTEGRATION

Accelerometers and gyroscopes of the INS systems are affected by biases that cause the measured position to drift over time. Such inertial drift can be compensated by integrating the inertial data provided by the INS with real time kinematic (RTK) or post-processed kinematic (PPK) GNSS data.

RTK/PPK is a carrier-phase-based differential GNSS technique involving a reference station located as close as possible to the rover (the moving platform in the GNSS jargon) to correct for ionospheric and tropospheric effects on the received signals. When the reference station and the rover are close to each other, ionospheric and tropospheric effects are approximately the same at the two receivers and cancel each other out with differential processing.

When the distance between reference station and rover (known as baseline) increases, the tropospheric effect at the two receivers is different and cannot be compensated. Since the ionosphere is a dispersive means, combination of different carrier signals is usually performed to estimate the ionospheric effect, at the cost of increased noise variance, and is effective when the baseline increases [11].

In this paper, we compare multiple PPK solutions¹ obtained with reference stations at different baselines (see Table

¹PPK processing performed with Novatel GrafNAV 8.70

1 and Table 2): the local GNSS receiver mounted in the field and two stations of the AGNES (Automated GNSS Network for Switzerland) augmentation network.

The integration of the inertial navigation data and the PPK data has been performed with an extended Kalman filter² followed by a Rauch-Tung-Striebel (RTS) smoother [12]. In a car-borne acquisition setup, the repeat-pass trajectories extracted from the RTS solution would be then used to focus the radar images via time domain back-projection [13, 14, 3].

| Station name | OALP | HABG | Local station |
|--------------|--|---------------------|--|
| Description | Static permanent GNSS stations of the AGNES network located in Oberalppass and in Hasliberg (CH) | | Static local non-permanent reference station |
| Baseline | ~20 km | ~20 km | < 10 m |
| Antenna type | Trimble TRM59800.00 | Trimble TRM59800.00 | Trimble TRM77971.00 |
| Altitude | 2139.53 m | 1147.92 m | 2000.37 m |

Table 1. Antenna type and description of the AGNES and the local reference stations with different GNSS baselines used for differential carrier-phase-based GNSS post-processing.

4. RESULTS

The analysis performed involves different PPK solutions and the corresponding integrated INS/GNSS solutions (RTS) for different acquisition and processing scenarios. The PPK solutions have been computed using single and dual-frequency processing (L1 and L1+L2 carrier signals) and different GNSS baselines (see Table 2). A ionosphere-free solution has been obtained via dual-frequency processing for the case involving the AGNES stations that are about 20 km away from the test site.

Figure 1 shows the estimated altitude of the PPK solutions. We show the altitude because it usually represents the component with the highest level of uncertainty. Since the platform is constrained by the rail, the time-varying error in the different scenarios can be assessed. During standstill positions, where static GNSS positioning is expected to outperform the one obtained during kinematic sessions, the estimated altitude shows time-dependent variations around its mean. The magnitude of such variations is clearly much smaller when the local GNSS reference station is used rather than the AGNES reference stations.

The superior precision of the local solutions can be better observed in Figure 2 that shows a box-plot of the PPK and the RTS altitude during the initial and the final standstill.

²INS/GNSS data integration performed with iMAR High Precision Short Time Tracking tool

| GNSS reference station | Carrier signal | Baseline | Legend entry |
|------------------------|----------------|----------|--------------|
| Local station | L1 | < 10 m | local_L1 |
| Local station | L1+L2 | | local_L1L2 |
| AGNES: OALP | L1+L2 | ~30 Km | OALP |
| AGNES: OALP + HABG | L1+L2 | | 2agnes |

Table 2. Configurations of GNSS reference stations and carrier signals used for PPK processing. Legend entry indicates the label names used in Figure 1 and Figure 3.

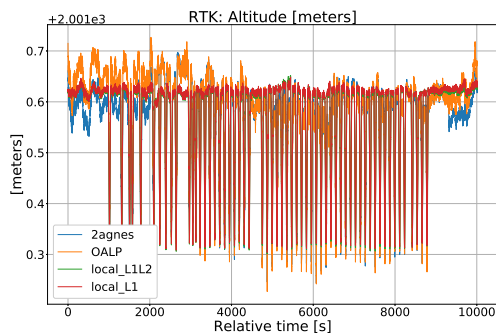


Fig. 1. Estimated altitude (WGS84) of the platform moving along the rail. Plots show the PPK post-processed solutions as indicated in Table 2. Initial and final position of the platform are in standstill (constant altitude). The intermediate repeated movements along the rail are relevant to L-band radar acquisitions.

Figure 3 shows the altitude difference of the AGNES and the local PPK solutions as well as the corresponding integrated RTS solutions. The smoothing effect of the Kalman filter is apparent. However, the long term position stability is still regulated by the PPK solution employed in the integration.

To quantify the trajectory estimation error during the repeat-pass acquisitions, we extracted and averaged, from the single-frequency local RTS solution, the individual trajectories relevant to the movement of the platform forth and back along the rail. Figure 4 shows the deviation of the altitude component of each individual repeat-pass trajectory from the average one. Most of the variation is contained within a range of 1 cm.

Considering the low speed and the low dynamic of the rail platform with respect to the car, the presented results likely represent a best-case scenario for trajectory estimation performance.

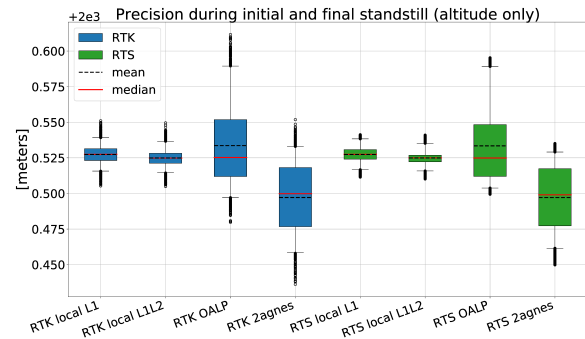


Fig. 2. Altitude precision of PPK and RTS solutions indicated in Table 2 during initial and final standstill positions. Mean and median are indicated. Whiskers indicate 5% and 95% percentiles.

5. CONCLUSIONS

In this paper we presented an analysis of the positioning performance attainable in the context of repeat-pass SAR measurements. We assessed the positioning performance of a platform carrying a SAR sensor using a navigation-grade inertial navigation system (INS) and a GNSS receiver moving along a rail. A second static geodetic GNSS receiver located few meters away from the platform has been used as local reference station for precise GNSS processing.

Although a rail-based system does not necessarily require a high-precision navigation system for radar processing, the constrained position is an ideal configuration to evaluate the trajectory estimation errors in a controlled setup.

The accuracy of the post-processed or real-time kinematic GNSS solutions shows significant influence on the final integrated INS/GNSS one. The global, long-term stability of the platform trajectory is regulated by the PPK solution and its accuracy varies consistently with the system configuration and the processing parameters.

A local GNSS reference station situated in the vicinity of the SAR platform offers superior positioning performance with respect to reference stations located kilometers away. Thus, the use of a local reference station is recommended in a car-borne or UAV-borne repeat-pass SAR measurements setup to improve the positioning performance and, hence, minimize residual interferometric phase errors.

6. REFERENCES

- [1] Rafael Caduff, Fritz Schlunegger, Andrew Kos, and Andreas Wiesmann, "A review of terrestrial radar interferometry for measuring surface change in the geosciences," *Earth Surface Processes and Landforms*, vol. 40, no. 2, pp. 208–228, 2015.

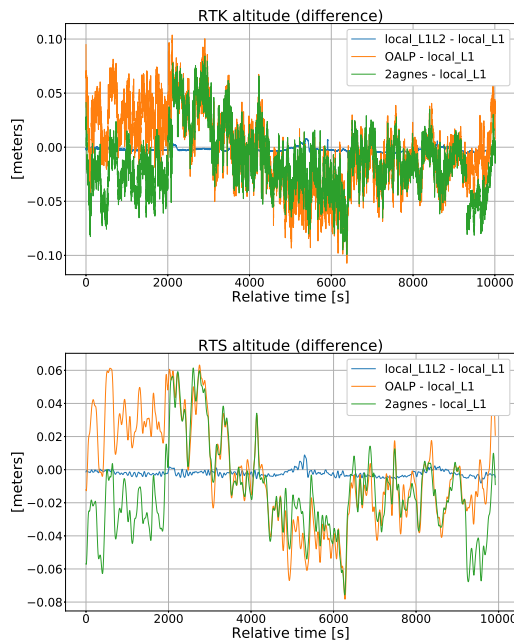


Fig. 3. Above: altitude difference between the PPK solutions processed with the AGNES and with the local GNSS reference stations. Below: corresponding altitude difference of the integrated GNSS/INS solutions obtained via RTS processing. See Table 2 for reference. During the repeat-pass acquisitions the platform is constrained to the rail (zero interferometric baseline) and it is possible to observe the time-varying error caused by the increased distance of the AGNES reference station.

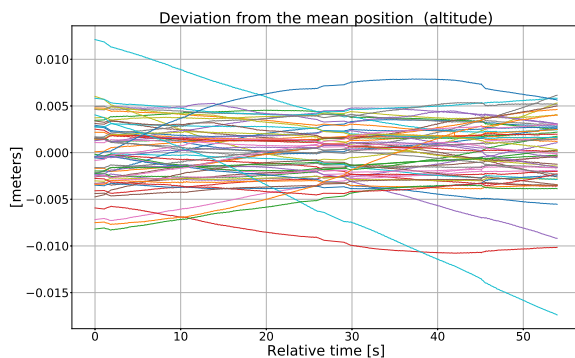


Fig. 4. Deviation from the average altitude of the altitude component of each repeat-pass trajectory extracted from the local single-frequency RTS solution. Although the radar platform exactly repeats its trajectory during the different passes along the rail, the estimated trajectories show time-dependent variations at centimeter-level.

- [2] Andrew K. Gabriel, Richard M. Goldstein, and Howard A. Zebker, "Mapping small elevation changes over large areas: differential radar interferometry," *Journal of Geophysical Research*, vol. 94, no. B7, pp. 9183–9191, 1989.
- [3] Othmar Frey, Charles L. Werner, Urs Wegmuller, Andreas Wiesmann, Daniel Henke, and Christophe Magnard, "A car-borne SAR and InSAR experiment," in *International Geoscience and Remote Sensing Symposium (IGARSS)*, jul 2013, pp. 93–96, IEEE.
- [4] Roberto Coscione, Irena Hajnsek, and Othmar Frey, "An Experimental Car-Borne SAR System: Measurement Setup and Positioning Error Analysis," in *IGARSS 2018 - 2018 IEEE International Geoscience and Remote Sensing Symposium*, 2018, pp. 6364–6367.
- [5] Othmar Frey, Charles L. Werner, Irena Hajnsek, and Roberto Coscione, "A Car-Borne SAR System for Interferometric Measurements: Development Status and System Enhancements," in *IGARSS 2018 - 2018 IEEE International Geoscience and Remote Sensing Symposium*, 2018, pp. 6508–6511.
- [6] Gianfranco Fornaro, "Trajectory deviations in airborne SAR: analysis and compensation," *IEEE Transactions on Aerospace and Electronic Systems*, vol. 35, no. 3, pp. 997–1009, jul 1999.
- [7] Gianfranco Fornaro, Giorgio Franceschetti, and Stefano Perna, "Motion compensation errors: Effects on the accuracy of airborne SAR images," *IEEE Transactions on Aerospace and Electronic Systems*, vol. 41, no. 4, pp. 1338–1352, 2005.
- [8] Pau Prats and Jordi J. Mallorqui, "Estimation of azimuth phase undulations with multiquint processing in airborne interferometric SAR images," *IEEE Transactions on Geoscience and Remote Sensing*, vol. 41, no. 6 PART II, pp. 1530–1533, 2003.
- [9] Pau Prats, Andreas Reigber, and Jordi J. Mallorqui, "Topography-dependent motion compensation for repeat-pass interferometric SAR systems," *IEEE Geoscience and Remote Sensing Letters*, vol. 2, no. 2, pp. 206–210, apr 2005.
- [10] Karlus A. Câmara De Macedo, Rolf Scheiber, and Alberto Moreira, "An autofocus approach for residual motion errors with application to airborne repeat-pass SAR interferometry," *IEEE Transactions on Geoscience and Remote Sensing*, vol. 46, no. 10, pp. 3151–3162, oct 2008.
- [11] B. Hofmann-Wellenhof, H. Lichtenegger, and E. Wasle, *GNSS – Global Navigation Satellite Systems: GPS, GLONASS, Galileo, and more*, Springer Vienna, 2007.
- [12] Herbert E. Rauch, C. T. Striebel, and F. Tung, "Maximum likelihood estimates of linear dynamic systems," *AIAA Journal*, vol. 3, no. 8, pp. 1445–1450, aug 1965.
- [13] Othmar Frey, Erich H Meier, and Daniel R Nüesch, "Processing SAR data of rugged terrain by time-domain back-projection," in *SAR Image Analysis, Modeling, and Techniques VII*, Francesco Posa, Ed., oct 2005, vol. 5980, p. 598007.
- [14] Othmar Frey, Christophe Magnard, Maurice Rüegg, and Erich Meier, "Focusing of airborne synthetic aperture radar data from highly nonlinear flight tracks," *IEEE Transactions on Geoscience and Remote Sensing*, vol. 47, no. 6, pp. 1844–1858, jun 2009.